Vision-Aided Inertial Navigation Using a Geomatics Approach

Fadi A Bayoud
Ecole Polytechnique Fédérale de Lausanne (EPFL)
Geodetic Engineering Laboratory (TOPO)

BIOGRAPHY

Fadi A Bayoud (Lebanese nationality) obtained a degree in Surveying Engineering in 1999 at the Aristotle University of Thessaloniki, Greece. In 2001, he received a M. Sc. in Geomatics Engineering at the University of Calgary with a specialization in GPS/INS gravimetry and Geoid Determination. Then, he joined the Geodetic Engineering Laboratory (TOPO) at the Ecole Polytechnique Fédérale de Lausanne (EPFL), Switzerland, as a Ph. D. student. His research activities include mobile mapping systems, sensors integration by Kalman Filter, robotics navigation and mapping, Geoid and Gravimetry.

ABSTRACT

This paper proposes and tests a method for bridging GPS outages during short and long periods with a vision-based inertial navigation. This method is similar to the Simultaneous Localisation And Mapping (SLAM), which is the problem of mapping the environment and at the same time using this map to determine the location of the mapping device. After 20 years of investigation, SLAM is still an open problem in the robotics community that searches a global, stable and efficient solution. This study falls in these trials, with a difference that it originates from the geomatics engineering perception of navigation and mapping. This paper solves the SLAM problem by integrating Photogrammetry and Inertial Measurement Unit (IMU) in a Kalman Filter. Briefly, from existing known features (ground control points, GCP) photogrammetric resection provides the position and orientation of the cameras that are integrated, after applying appropriate systems transformations, with the IMU data to produce a filtered position, which by its turn is used in the intersection to map more surrounding features, that are used as GCPs in the next epoch. Our methodology is presented, differences with other solution are pointed out, and numerical tests are discussed.

Keywords. Navigation. Photogrammetry; Least-Squares Adjustment; Kalman Filter; SLAM.

INTRODUCTION

In terrestrial based mobile mapping systems, GPS outages are frequent and depending on the IMU quality, these outages can cause loss inaccuracy that is impossible to overcome if other positioning sensors are not available. The method proposed here can be considered as either a continuous positioning update or a bridge to GPS gaps. This method is similar to the Robotics Simultaneous Localisation And Mapping (SLAM). In what follows, the analysis will be carried out considering that GPS is not available, during a period lasting several seconds to several minutes.

Robotics Simultaneous Localisation And Mapping (SLAM) is the problem of mapping the environment surrounding the robot and at the same time using this map to determine the location of the robot (Csorba, 1997; Newman 1999). Navigation and mapping systems are the core elements of SLAM, without which an exploring robot cannot do its job. The applications of self-navigating – exploring – robots are abundant, but one of the most important is: going to and exploring places where no man is safe to do. A map of the surrounding environment of the robot and a navigation system are essential for the robot to perform manoeuvres and in turn to complete its mission. These robots do not reach the perfection by only having a good navigation and mapping system. The navigation and mapping system is only a part of an integrated system that combines control with artificial intelligence, dynamics, sensing, vision, learning, estimation methods, etc. It is even hard to tell which of these is more important since they all work as a group, benefiting from each others' supremacy.

Traditionally, terrestrial robotics SLAM is approached using LASER scanners to locate the robot relative to the structured environment and to map this environment at the same time. LASER scanners have shown to be a very good tool where the accuracy of localisation is within the centimetre level. However, outdoors robotics SLAM is not feasible with LASER alone due to the absence of

stereotypic features and environment's roughness. Therefore, different tools have to be used.

Recently, the use of visual methods, integrated with inertial sensors, has gained an interest. These visual methods rely on exploitation of one or more cameras (or video). Yet, no clear indication about the mapping methods or integration algorithms is explicitly illustrated; one can consult the Journal of Robotics Systems (2004). Jung (2003) has used vision motion estimation to perform SLAM. His method relies on linking the pixel's motion rate on the images with the displacement of the robot. However, this filter has to run at very high rates and in case of vision loss, no other means to re-locate the robot is available.

These particular solutions use a single Kalman Filter with a state vector containing the map and the robot coordinates. This introduces high non-linearities, large state vector as well as other complications to the filter, which needs to run at high rates (20 Hz) with simplified navigation models. A classical tool for mapping is Photogrammetry, where sequence of stereo-images are captured and self-oriented. As for the navigation systems, the coupling of Inertial Navigation System (INS) and Global Navigation Satellite Systems (e.g., the GPS) is indispensable. In addition, photogrammetry can also be used for localisation – positioning.

In this paper, a mobile mapping system to solve SLAM is introduced – independent of the GPS/INS integration – by employing two CCD cameras and one IMU. Two filters are used in parallel: the Least-Squares Adjustment (LSA) for mapping and the Kalman Filter (KF) for navigation. Conceptually, the outputs of the LSA photogrammetric resection (position and orientation) are used as the KF external measurements. The filtered position and orientation are then employed in the LSA Photogrammetric intersection to map the surrounding that is used (as control features) for the resection in the next epoch. In this manner, the KF takes the form of a navigation filter only, with a state vector containing the corrections to the navigation parameters. This way, the mapping and localisation can be updated at low rates (1 to 0.5 Hz) and more complete modelling of sensor errors is applied.

While photogrammetry alone can solve SLAM, the presence of an IMU is significant for automated feature detection and orientation. Moreover, the IMU is indispensable in cases where images cannot be used for reasons of visibility and when certain manoeuvres do not guarantee knowledge of the environment; e.g. when the robot or vehicle captures images of an unknown environment. To use photogrammetry to solve SLAM, full automation is required, which is still not fully achieved.

Many attempts are directed towards the automation of photogrammetry; this goal has been still falling short due to the need of high level of artificial intelligence.

In the next section, the methodology to solve the SLAM problem by photogrammetry and IMU is introduced. The third section discusses briefly the photogrammetric mathematical model, the angular transformations and lever arm corrections that link the cameras' outputs with those of the IMU. Kalman Filter is shortly presented in section four. A numerical investigation is described and analysed in section five. Finally, conclusions are drawn in the last section.

A METHODOLOGY FOR COMBINING PHOTOGRAMMETRY AND IMU OUTPUTS

The methodology followed in this research is different from the traditional SLAM solution pursued by the Robotics community. In the following, there will be two separate filters; the first is the Least-squares Adjustment (LSA) filter that will do the mapping and localisation by photogrammetry; the second is the Kalman Filter that performs the localisation by optimally integrating the localisation provided by the LSA with the IMU outputs.

The employed Kalman Filter (KF) is very similar to that used in the INS/GPS navigation. But instead of using the GPS positioning and velocity updates, the LSA outputs from photogrammetric resection, the Exterior Orientation parameters (EOP), position and orientation, will be used as updates. In this way, the KF is a navigation-only filter that: i) operates at the frequency of the update (e.g., 1 or 0.5 Hz), and ii) its state vector size is kept relatively small (e.g., 15 states) with homogeneous states that guarantee rapid convergence.

This procedure requires certain points to consider:
- Recursive LSA: the LSA solution of the epoch $k-1$ is used as observations for epoch k,
- Correlations between measurements and unknowns are carried from one epoch to the other.

Before starting, we need to initialise the system by defining its position and orientation with respect to a well-defined mathematical reference frame that has a physical meaning. This is important when the SLAM is solved on a global scale. This is called Georeferencing. The Georeferencing can be done in two ways:
1. Initialisation with GPS/INS, which demands open skies for the GPS signal, or
2. Initialisation with resection, which demands the existence of sufficient Ground Control Points (GCP) at the beginning of the survey.
3. Standing on a known point, and stable IMU alignment.

In the first case, open sky for the GPS is vital. The GPS/INS gives us the position and attitude of the IMU, which – after applying the lever arm and angles transformation – yield the EOP of the two cameras. As for the second case, at least three GCPs are required for the determination of the position and attitude of the two cameras by resection. Having the initialisation properly done, the vehicle moves and starts to map and localise itself as portrayed in chart of Figure 1 that shows the algorithm concept.
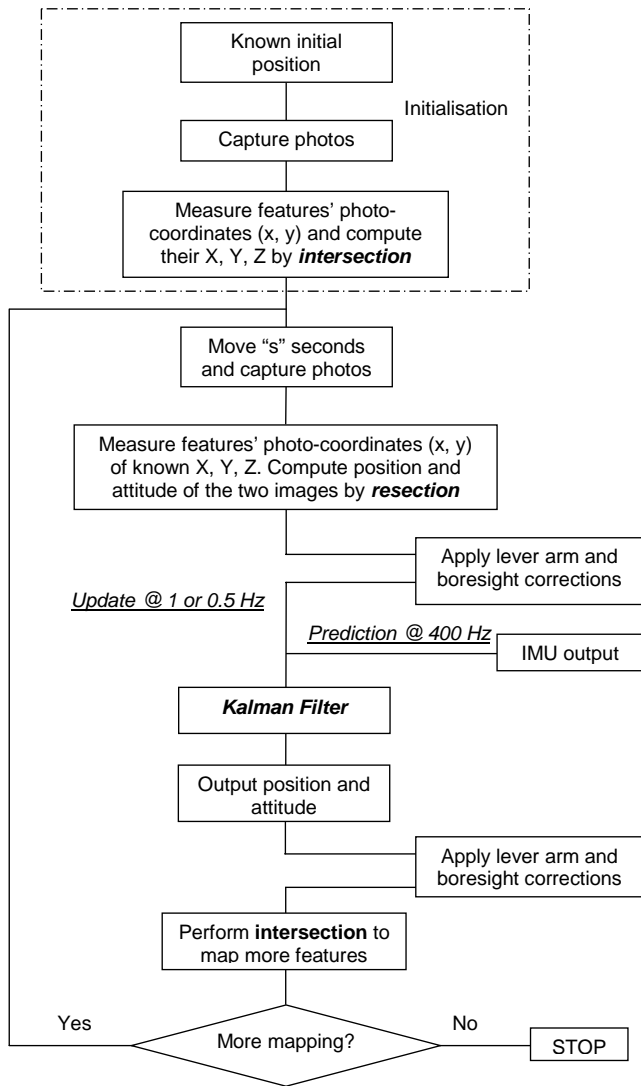

Figure 1: Flowchart of the Photogrammetric and IMU integration

The data flow can be depicted as follows:

Initialisation:
1. Position and attitude of the two cameras considered as known
2. Intersection is employed to map features

After mapping enough features:
1. Vehicle moves.
2. Resection computes the cameras' EOP by LSA using the features mapped from the previous cameras' location. (IMU predicted EOP can be used for feature extraction as well.)
3. Lever-arm and angles transformation (boresight) are applied to the EOPs to determine the IMU's position and attitude.
4. IMU outputs and IMU position and orientation derived from resection are integrated in a KF to compute filtered position and attitude of the current system location.
5. Lever-arm and angles transformation (and boresight) are applied to the filtered position and attitude to determine the EOP of the cameras.
6. Intersection is used to map more objects by LSA from the current location.
7. Vehicle moves and algorithm repeats.

Stages 3 and 5 are of great importance in the process of navigation and mapping, for the following facts (Figure 2):
- The cameras and the IMU are separate in space
- The outputs of photogrammetry and IMU belong to different reference systems; photogrammetry functions either in the camera space or object space and the IMU's outputs are in the body frame.
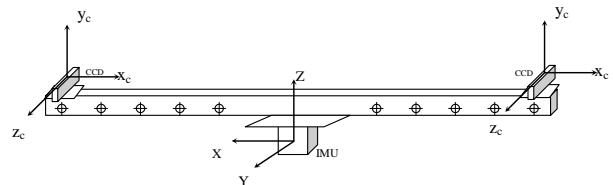

Figure 2: Mounting of the cameras and IMU

PHOTOGRAMMETRIC MATHEMATICAL MODEL, ANGLE TRANSFORMATION AND LEVER ARM

Mathematical properties governing the relationship between the image and the objects are shown in Figure 3. The perspective centre, the object and its image are

collinear, yielding a functional model called the co-linearity equation:

$$x = x_0 - c \frac{R_{11}(X-X_0)+R_{12}(Y-Y_0)+R_{13}(Z-Z_0)}{R_{31}(X-X_0)+R_{32}(Y-Y_0)+R_{33}(Z-Z_0)}$$

$$y = y_0 - c \frac{R_{21}(X-X_0)+R_{22}(Y-Y_0)+R_{23}(Z-Z_0)}{R_{31}(X-X_0)+R_{32}(Y-Y_0)+R_{33}(Z-Z_0)}$$

(1)

where x, y are the photo-coordinates in the image frame, X, Y, Z are the 3-D Coordinates in the object frame, c is the focal length of the camera, X_0, Y_0, Z_0 are the 3-D Coordinates of the camera's perspective centre in the object frame, x_0, y_0 are the photo-coordinates of the projection of the perspective centre to the image plane, (theoretically, this projection point has to coincide with the principle point, which is the centre of the image frame, but in reality, it does not) and R_{ij}'s are the elements of the rotation matrix between the image and object frames, $\mathbf{R_m^c}$.
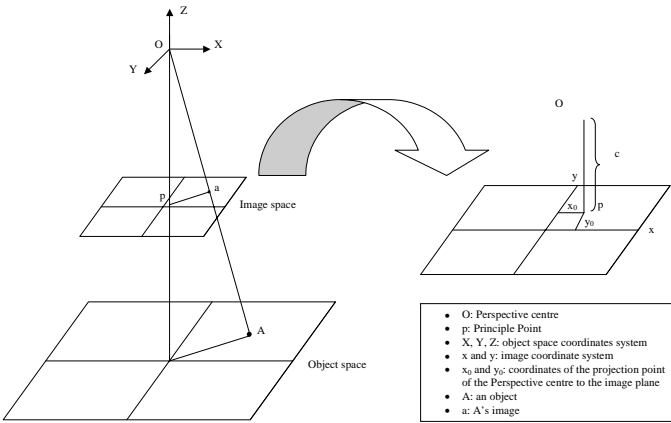

Figure 3: General Image Geometry

Equations 1 describe the fundamental mathematical model for photogrammetric mapping, where it reveals the relationship between the image and the object coordinate systems. With this model, one can solve the basic problems of photogrammetric mapping, namely: resection and intersection:

- **Resection**: In resection, the position and attitude (EOP) of an image are determined by having a set of at least three points with known coordinates in the object frame as well as in the image frame; these are the GCPs.
- **Intersection**: In intersection, two images, with known EOPs, are used to determine the coordinates in the object frame of features found on the two

images simultaneously, employing the principle of stereovision.

In principle, photogrammetry alone can be used to solve SLAM by employing recursively resection and intersection. This was analysed by a previous publication, Bayoud et al (2004); however, there are important shortcoming of such approach as mentioned in the Introduction.

Angles transformation and lever arm

The angle transformation applied in Stage 3 (going from resection to KF), is used to transform the orientation output of the resection from the mapping/camera frame to the earth/body frame to be consistent with the inertial output and KF states

$$\mathbf{R_b^e} = \mathbf{R_m^e} \left(\mathbf{R_m^c}\right)^{\mathbf{T}} \mathbf{T_{b^*}^c} \mathbf{R_b^{b^*}}$$

(2)

Where $\mathbf{T_{b^*}^c}$ is the rotation matrix between IMU and camera frames and depends on the definition of the axes (Figure 3), $\mathbf{R_b^{b^*}}$ is the boresight that contributes for the mounting imperfections, $\mathbf{R_b^e}$ is the rotation matrix between IMU body frame and Earth-Centred-Earth-Fixed (ECEF) frame, and $\mathbf{R_m^e}$ is the rotation matrix between ECEF and mapping frames.

The angle transformation applied in Stage 5 (going from KF to intersection) is used to transform the output of the inertial and KF to the camera's reference frame to perform the mapping. This is well documented in the relevant literature because it is the classical way of image direct-Georeferencing by GPS/INS (Skaloud and Schaer, 2003). The transformation is:

$$\mathbf{R_m^c} = \mathbf{T_{b^*}^c} \mathbf{R_b^{b^*}} \left(\mathbf{R_b^e}\right)^{\mathbf{T}} \mathbf{R_m^e}$$

(3)

The lever arm is divided as well into two parts depending on whether the process goes from resection to KF or from KF to intersection. In the first case, resection gives the coordinates of the cameras in the mapping frame. To these, the leverarm is added to obtain the coordinates of the IMU in the mapping frame, and then to transformed to the ECEF frame. Having the coordinates of the IMU, computed from resection, in the ECEF frame, they update the KF to determine the filtered position of the IMU. This process can be shown in four steps:

Step one:

$$I_j{}^m = \mathbf{R}_{c/j}^m I_j{}^c \tag{4}$$

where $I_j{}^c$ is the leverarm in the camera frame, $I_j{}^m$ is the leverarm in the mapping frame, $\mathbf{R}_{c/j}^m$ is the rotation matrix between the camera and mapping frame for camera j (Left or Right).

Step two:

$$\mathbf{X}_{IMU/j}{}^m = \mathbf{x}_{cam/j}{}^m + I_j^m \tag{4}$$

Where $\mathbf{x}_{cam/j}{}^m$ is camera j coordinates in the mapping frame (from resection), $\mathbf{X}_{IMU/j}{}^m$ is IMU coordinates in the mapping frame.

Step three:

$$\mathbf{X}_{IMU/j}{}^e = \mathbf{R}_m^e \; \mathbf{X}_{IMU/j}{}^m \tag{5}$$

Where $\mathbf{X}_{IMU/j}{}^e$ are the coordinates of the IMU in the ECEF frame computed from camera j.

Step four:

$$\mathbf{X}_{IMU}{}^e = KF\left(\mathbf{X}^e, \mathbf{X}_{IMU/L}{}^e, \mathbf{X}_{IMU/R}{}^e\right) \tag{6}$$

Where $\mathbf{X}_{IMU}{}^e$ are the Kalman filtered (KF-ed) coordinates of the IMU in the ECEF frame, $\mathbf{X}^e$ are the coordinates of the IMU in the ECEF frame computed from the mechanisation equations, $KF\left(\mathbf{X}^e, \mathbf{X}_{IMU/L}{}^e, \mathbf{X}_{IMU/R}{}^e\right)$ is the Kalman filter output with $\mathbf{X}^e$ as prediction, and $\mathbf{X}_{IMU/L}{}^e$ and $\mathbf{X}_{IMU/R}{}^e$ as updates.

The second process is the classical procedure in Georeferencing and is the reverse of the first: The KF gives the filtered position of the IMU in the ECEF frame. To these the leverarm is added to determine the camera in the ECEF frame. The result will be transformed to the mapping from to perform the intersection. This process can also be explained in four steps:

Step one:

$$I_j^b = \mathbf{R}_c^b . I_j^c \tag{7}$$

Where $I_j{}^b$ is the leverarm in the body frame.

Step two:

$$I_j^e = \mathbf{R}_b^e . I_j^b \tag{8}$$

Where $I_j{}^e$ is the leverarm in the ECEF frame.

Step three:

$$\mathbf{X}_{CAM/j}{}^e = \mathbf{X}_{IMU}{}^e + I_j^e \tag{9}$$

Where $\mathbf{X}_{IMU}{}^e$ is the IMU position in the ECEF frame determined by KF, $\mathbf{X}_{CAM/j}{}^e$ is camera j position in the ECEF frame.

Step four:

$$\mathbf{X}_{CAM/j}{}^m = \mathbf{R}_e^m \; \mathbf{X}_{CAM/j}{}^e \tag{20}$$

Where $\mathbf{X}_{CAM/j}{}^m$ is the Kalman filtered position of camera j in the mapping frame.

$\mathbf{X}_{CAM/L}{}^m$ and $\mathbf{X}_{CAM/R}{}^m$ are used in intersection to map more features.

Leverarm and Boresight calibration

The concept of the boresight $\mathbf{R}_b^{b^*}$ determination is well documented in the relevant literature (Bäumker et al., 2001; Skaloud and Schaer, 2003). In this work, an indirect procedure was followed to determine the two boresight matrices and two leverarm vectors of the left (L) and right (R) cameras. In the frame of the work carried out at the Geodetic Engineering Laboratory, a mapping system with a high-definition digital camera (will be named as "H") is well calibrated with respect to the IMU with known boresight and leverarm; to this system, the two CCDs were added (Figure 4). The boresight and leverarm of the two CCDs were first calibrated with respect to the high-definition digital camera by determining the EOP of the three cameras in three different locations. Then, once average boresight and leverarm were computed, the link between the two CCDs and the IMU were directly made through the already known boresight and leverarm between the digital camera and the IMU. The estimated accuracy of the EOP, boresight and lever arm between the cameras are shown in Tables 1 and 2.

Table 1: Estimated Angle and boresight accuracy (arcmin) (L=Left CCD, R=Right CCD, H=High Definition Camera)

		Pitch	Azimuth	Roll
EOP	L	1.7	1.4	1.3
	R	1.8	1.5	1.1
	H	0.5	0.4	0.3
Boresight	L to H	3.50	6.26	2.84
	R to H	0.91	2.80	3.27

Table 2: Estimated cameras position and leverarm accuracy (cm)

		X	Y	Z
EOP	L	0.3	0.2	0.3
	R	0.3	0.2	0.3
	H	0.1	0.1	0.1
leverarm	L to H	1.0	1.6	1.0
	R to H	0.6	1.0	0.3
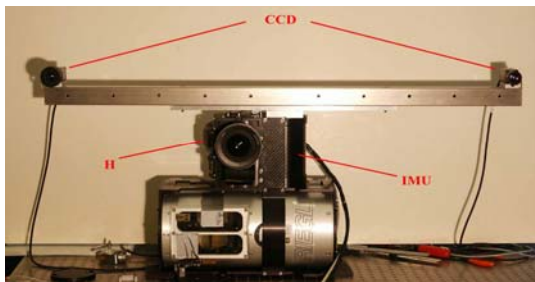
Figure 4: The system

DATA INTEGRATION VIA KALMAN FILTER

The navigation Kalman Filter can link either the IMU measurements (orientation rates and accelerations) or the integrated values (coordinates, velocity, orientation) with external measurements. In open spaces, GPS measurements usually play the role of external measurements. In areas with limited GPS signal, other sensors – like odometer, compass, barometer, etc. – are used. Here, we take for the KF external measurements the output of the photogrammetric resection; these are the Coordinates Update (CUPT) and Attitude Update (AUPT). In addition, Zero-Velocity Updates (ZUPT) can also be used as measurements. This kind of updates allows adopting loosely coupled integration, which is easier to implement.

Since there are two cameras, two datasets of external measurements are available; one is the EOP of the left camera and the other is the EOP of the right camera. There are two possibilities for this integration. The first possibility is to take the average of the two EOPs. The second considers the two EOP as two independent correlated updates. The difference between the two possibilities is reflected in the size and shape of the measurements' vector, co-variance matrix, and design matrix. In this paper, we are applying the first possibility, while future publications will consider the second. For details concerning the mechanisation equations of inertial measurements and error modelling in Kalman Filter, the reader can consult Schwarz and Wei (2000), Titterton and Weston (1997).

NUMERICAL TESTS

Two tests were performed indoors in a controlled environment to initially evaluate the methodology and validate the software; the results were encouraging to carry out extensive outdoor testing. Two CCD cameras (SONY XC-55 with a 6 mm lens) and an LN-200 IMU were used as instruments. Along, there were a synchronisation pulse, a Matrox Meteor-II/Multi-Channel frame grabber and a screen, IMU data acquisition box developed at the EPFL-TOPO (Skaloud and Viret, 2004), a laptop, and the power supply. The image grabbing was carried out at every second and was properly synchronised with the IMU via a synchronisation pulse. After a couple of minutes of static inertial initialisation, the vehicle moved and started taking images. Out of a set of few tens of images, a set of 14 images in a 7 stereo-pairs with 2 to 3 to seconds apart, were chosen to minimise the photogrammetric processing effort. This means that the Kalman Filter update will occur every two to three seconds. Figure 5 portrays a sample of the images. Beforehand, there was a set of GCPs for the initialisation; after that, the SLAM took over to map more features and locate the cameras.

Two initialisation methods were tested:
- Initialisation by resection
- Initialisation by gyro-compassing

Although photogrammetric resection should provide very accurate roll and pitch, it was found in this test that these values were not consistent with the roll and pitch derived by gyro-compassing. (It was found later on that there is a problem in the boresight estimation.)

The inaccurate initialisation from photogrammetric resection caused the IMU-only solution to diverge rapidly if no updates are provided, which is clearly seen in the innovation information for the second epoch (Figure 6). The update at position 2 was made by GCPs as well due to the discontinuity in visibility between images 1 and 2. After that update, the Kalman Filter succeeded to correct the initial misalignments and position uncertainties and

the navigation solution started to converge within the limits of the accuracy of the resection.
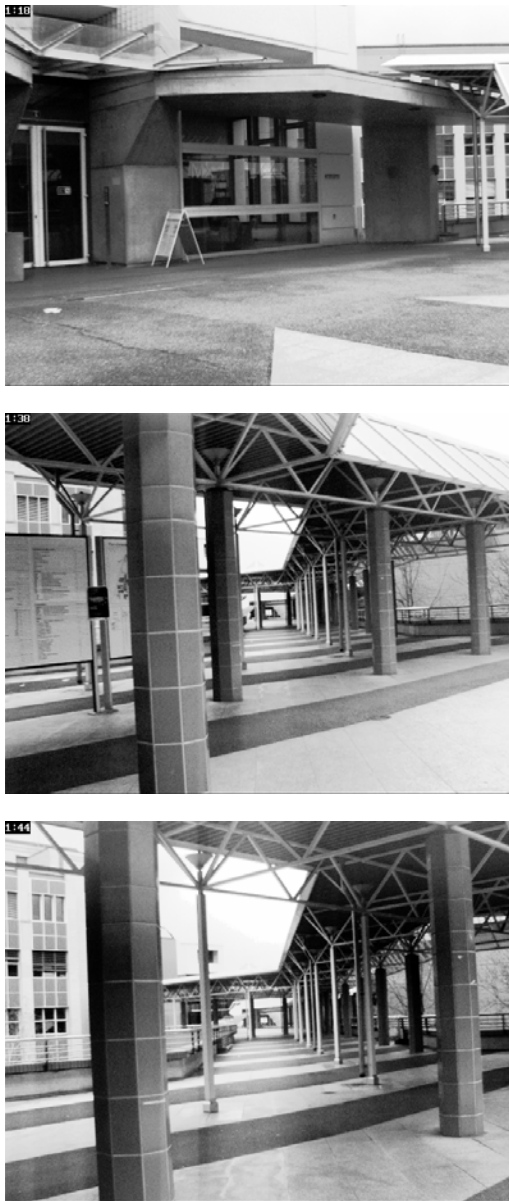

Figure 5: Image examples of the first set

When gyro compassing is performed to compute the initial attitude, the convergence was faster and the navigation solution was better as can be seen in Figure 7. The predicted position at the second epoch is very close to the update and the rest of the points are more consistent with their updates than those of Figure 6. It is logical to see that at epochs 6 and 7 the innovation becomes worse; this is because the resection at this time completely depends on the newly mapped features.

It is worthwhile to note the stability in the z-channel – with almost the same results regardless of the initialisation method used – where after the third epoch the innovation does not exceed few centimetres (Figure 8). It is rarely seen that the innovation of z-channel is better than that of the horizontal channels. However, in this particular case the initial misalignment is the dominant source of errors causing the X and Y components to drift; this analysis comes from the deduction that the Z-component of the IMU (its weak component) is very consistent with the Z-component of resection (the strong photo component).

This test highlights the importance of good cameras' set-up. When working outdoors, the operator cannot control the features' quality, where many of them are of unclear visibility and/or far away from the cameras. The images can be seen in Figure 5; although they show to be unambiguous, once fine targets are sought, problems start to appear. Looking for example at the third image of Figure 10, by zooming in (see Figure 6), one can see the difficulty in finding a fine target to use. This reduces the photo-coordinates quality and thus the whole system is affected. First, the initialisation becomes of insufficient accuracy, and the positioning and orientation determination develop into inaccurate input to perform reliable update for the Kalman Filter.

According to the photogrammetric theory and simulations done before, the depth (X and Y components) is geometrically weak because of the small stereo base of 1 meter. Twenty-one points were used as checkpoints throughout the survey, whose validation and accuracies are shown in Figure 9 with the largest error belonging to those points that are the more than 15 meters from the stereo-base. Here also one can see the accurate mapping of the Z-component.
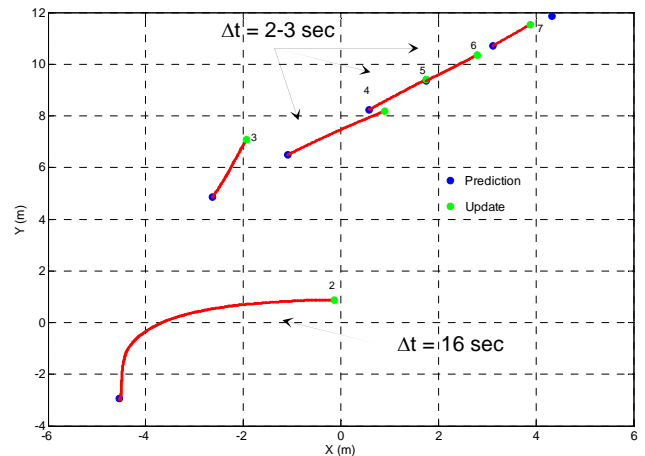

Figure 6: Vehicle planimetric trajectory showing the differences between the prediction and update when initialised with photogrammetry (innovation)
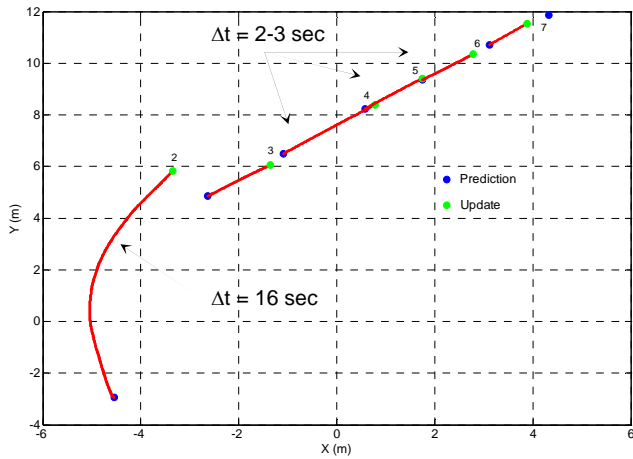
Figure 7: Vehicle planimetric trajectory showing the differences between the prediction and update when initialised with gyro-compassing (innovation)
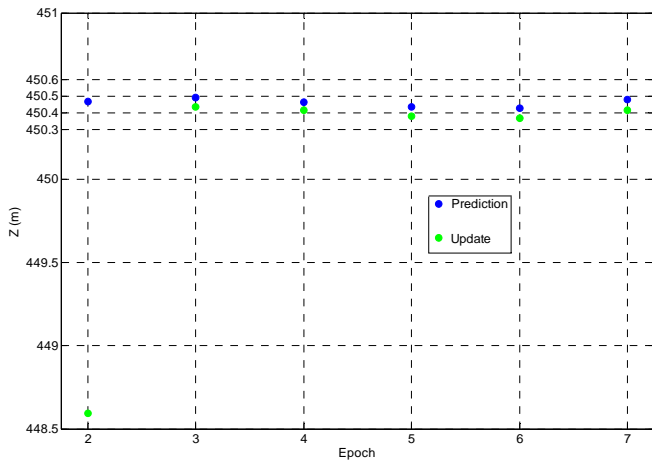

Figure 8: Vehicle vertical trajectory showing the differences between the prediction and update (innovation)
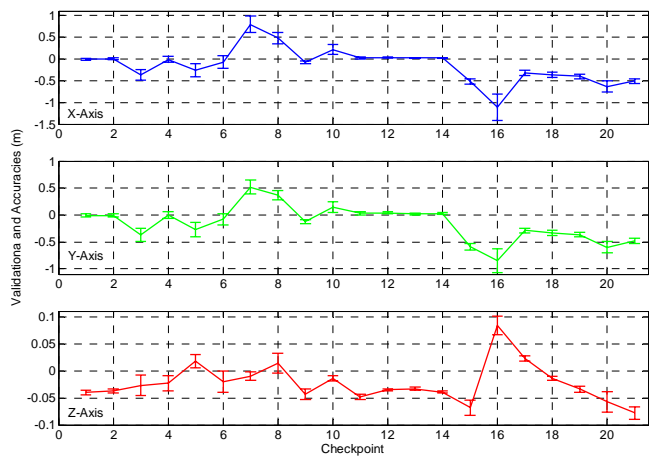

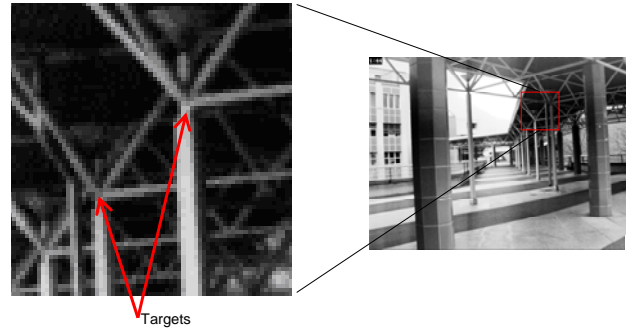**Figure 9: Validation and accuracies of the 21 checkpoints**

Figure 10: An example of the poor quality of the images once zoomed to find targets to map

CONCLUSIONS AND FUTURE WORK

In this paper a vision-aided inertial navigation system is presented. An integration procedure between an IMU and photogrammetry/cameras was developed and tested. The outputs of a pair of cameras are used first to localise the vehicle; this position is then used as an external measurements in a Kalman Filter whose prediction are the outputs of an IMU. The Kalman filtered position is used, then, with the outputs of the two cameras to perform the feature mapping in a least-squares adjustment filter. The procedure is called SLAM; a term borrowed from the robotics community and is investigated here using a Geomatics Engineering approach.

Conceptually, the data integration between both sensors is done in a loosely-coupled Kalman Filter. The algorithmic part of the filter is far from being simple and routine implementation needs an understanding of system control, data handling, and priority managing. Post-processing was done in the preliminary step by software that was written for the purpose of his work.

The conceptual advantages of using IMU/photo compared to only photos SLAM are considerable:
- Image sequences with limited or no overlaps do not halt the mapping
- IMU predicted EOP allows faster and more reliable automated feature extractions
- Increased robustness and accuracy

The numerical test and results were promising and show the practical feasibility of our procedure. What is left to be done is a detailed study of the stochastic modelling and error propagation needed to produce optimal results. The effect of the boresight uncertainty is clearly seen and should be re-estimated. Moreover, an outdoor survey with GPS will be carried out to further test the methodology.

An important remark from this work is the need of synergy between different specialisation for the

advancement of science and technology. In this work two distinct sciences were combined, from which an apparent benefit for both become clear.

REFERENCES

1. Bäumker M., F. J. Heimes (2001): New Calibration and Computing Method for Direct Georeferencing of Image and Scanner Data Using the Position and Angular Data of an Hybrid Inertial Navigation System. OEEPE Workshop, Integrated Sensor Orientation, Sep. 17-18, 2001; Hanover.
2. Csorba M. (1997): Simultaneous Localisation and Map Building. Ph.D. Thesis. Robotics Research Group, Department of Engineering Science, University of Oxford, 1997.
3. Newman P. M. (1999): On the Structure and Solution of the Simultaneous Localisation and Map Building Problem. Ph.D. Thesis, Australian Centre for Field Robotics, The University of Sydney, 1999.
4. Journal of Robotics Systems: Volume 21, Issues 1 and 2, January and February 2004, http://www3.interscience.wiley.com/cgi-bin/jhome/35876. Wiley Periodicals, pp 1-94.
5. Jung I K (2003): Simultaneous Localisation and Mapping in 3D Environments with Stereovision. PhD Thesis. CNRS-LAAS Report N° 04132, France.
6. Skaloud J., P. Schaer (2003): Towards a More Rigorous Boresight Calibration. ISPRS International Workshop on Theory, Technology and Realities of Inertial/GPS/Sensor Orientation, Commission 1, WG I/5, 2003.
7. Skaloud J. and P. Viret (2004): GPS/INS Integration: From Modern Methods of Data Acquisition to New Applications, European Journal of Navigation, Nov. 2004: 60-64.
8. Bayoud F. A., J. Skaloud, and B. Merminod (2004): Photogrammetry-Derived Navigation Parameters for INS Kalman Filter Updates. XXth ISPRS Congress 2004. Commission V, WG V/2, 2004.
9. Schwarz K. P. and M. Wei (2000): INS/GPS Integration for Geodetic Applications, Lecture Notes ENGO 623. Department of Geomatics Engineering, University of Calgary, Canada, 2000.
10. Titterton D. H. and J. L. Weston (1997): Strapdown Inertial Navigation Technology, Peter Peregrinus Ltd., 1997.